Deterministic Sampling on the Circle Using Projected Cumulative Distributions

Daniel Frisch and **Uwe D. Hanebeck**

Intelligent Sensor-Actuator-Systems Laboratory (ISAS)
Institute for Anthropomatics and Robotics
Karlsruhe Institute of Technology (KIT), Germany
daniel.frisch@ieee.org, uwe.hanebeck@ieee.org

Abstract—We propose a method for deterministic sampling of arbitrary continuous angular probability density functions. With deterministic sampling, good estimation results can be obtained with a much smaller number of samples than with the commonly used random sampling. The Unscented Kalman Filter also uses deterministic sampling, but takes a very small number of samples. Our method can draw an arbitrary number of deterministic samples, improving the quality of state estimation. Conformity between the continuous density function (reference) and the Dirac mixture density, i.e., sample locations (approximation), is established by minimizing the distance of the cumulatives of dozens of univariate projections. In other words, we compare density functions in Radon space.

I. INTRODUCTION

A. Considered Problem

In this work, we consider the problem of deterministic sampling of arbitrary continuous densities on the circular domain with an arbitrary number of unweighted samples.

B. Context

State estimation or control techniques for nonlinear systems often use samples (or particles) to represent the occurring densities. Obtaining unweighted discrete samples (on continuous domains) from a continuous probability density function (PDF) is, therefore, an important module in many state estimators and controllers. The "brute force" approach, often used to obtain ground truth for reference, is Monte Carlo Sampling with large numbers of entirely random samples. There are universal but rather slow random sampling methods like Metropolis-Hastings [1], and faster methods that are specialized for certain densities like the von Mises-Fisher distribution [2]. Acceptance-rejection methods [3], [4] are always an option as well, their efficiency depending on whether a good proposal distribution is available. The uniform proposal that is predestined for arbitrary density functions would become inefficient for "narrow" densities.

Ideal for filtering are also weighted particles on a regular grid, but likewise expensive, especially in higher dimensions. In the non-compact Euclidean space, the region with non-negligible probability density must be tracked and filled with a floating grid for this purpose [5]. On closed Riemannian manifolds such as the circle [6], the sphere [7], or the torus [8], it is possible to fill the entire domain with a regular grid, but expensive to extend to a high number of dimensions. To optimize computational complexity, it can be advantageous to
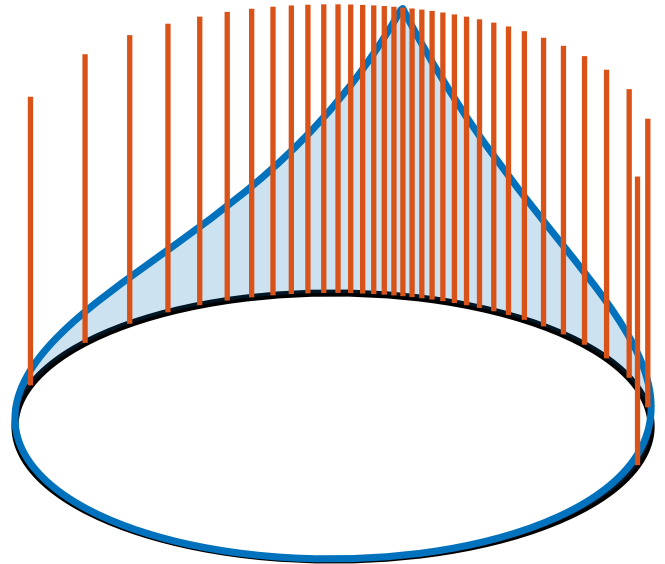
Fig. 1: Wrapped Laplace Distribution (blue) on the circular domain (black) with proposed deterministic sampling for 35 samples (red).

use a parametric representation that efficiently approximates a complicated likelihood or density function [9]. Similar ideas have been proposed also for Riemannian manifolds like the torus [10].

While parametric density representations can be convenient, it is often difficult to update the parameters when the system model is nonlinear. Therefore, many nonlinear parametric filtering algorithms use some kind of numerical integration internally [11]. In embedded systems subject to real-time constraints and limited memory, the number of evaluation points for numerical integration should be rather small.

C. State-of-the-art

Moment-based deterministic sampling of normal densities in the Euclidean domain using a very small number of samples is the basis of the Unscented Kalman Filter (UKF) [12], [13]. Its efficient concept has successfully been transferred to the circular domain [14], [15], however, inheriting equivalent limitations (only a small number of samples, only specific types of densities). Using higher-order moments, the number of samples can be increased to five [16] and multiples of

four (plus one) with superposition techniques [17]. UKF-like sampling methods are easily applied to higher-dimensional directional estimation for orientations on the hypersphere [18], [19], for multivariate circular estimation on the torus [20], and for dual quaternions on special Euclidean groups [21], [22], general Lie groups [23], or arbitrary Riemannian manifolds [24], [25] – all without an exponential increase of the computational cost.

The question that arises is how to make deterministic sampling more flexible, i.e., provide more samples than UKF-like schemes, but avoid Cartesian products. One way to achieve this is based on the Localized Cumulative Distribution (LCD) and a modified Cramér-von Mises distance. The LCD transforms any density, either continuous or Dirac mixture (DM), to a continuous representation via kernel convolution. The modified Cramér-von Mises distance is basically an L^2 norm of the difference of densities [26] but additionally averages over all kernel widths. LCD and modified Cramér-von Mises distance together yield a distance measure between continuous and DM densities in any combination [27], which has been successfully applied in the Euclidean domain [28], especially for Gaussian densities, where pre-computed samples are taken from a library during run time [29], [30].

Early adaptions to directional estimation applied the LCD in the Euclidean tangent space of the density's mean, placing samples on the coordinate axes only [31] or distributing them in the entire tangent space [32]. Direct application of the LCD on non-Euclidean manifolds has been performed for sample reduction (DM to DM approximation) on the sphere [33], the hypersphere [34], and for dual quaternion sample reduction in the special Euclidean group SE(2) [35]. Unfortunately, this method cannot easily be applied to arbitrary density functions and manifolds, because the involved integrals often do not exist in closed form. For the special case of the von Mises-Fisher density, there is also a very efficient deterministic sampling method that places samples on an arbitrary number of "beams" in a star-like arrangement [36], [37]. It is very fast and more flexible than UKF-like placement, but the star-like arrangement does not always cover the state space homogeneously and purely according to the density function.

There are many applications for angular state estimation and control on Riemannian manifolds, with potential applications for deterministic sampling enabling more efficient implementation. An interesting application is odor source localization [38], [39] because the angular measurements of odor sources are very uncertain, thus the naïve estimation in the Euclidean tangent space would be particularly insufficient here. The same holds for acoustic source localization and tracking [40], [41], [42]. Magnetometers and gyroscopes yield angular measurements as well, and sensor fusion methods should respect that [43]. Advanced deterministic sampling methods that fit into this context have already been successfully applied to wavefront orientation estimation [44] and visual Simultaneous Localization and Mapping [45]. Of course, depending on the sensor capabilities and the occurring motions, measurement and state spaces can be spheres S^2 or

hyperspheres S^N, where the circular solution we are going to present here would not be sufficient.

Yet, this does not lessen the importance of filtering or sampling approaches specifically optimized for the S^1 domain only. Applications with circular estimation problems include: 1) Phase estimation in transmitted electromagnetic signals [46]. 2) Reflectometry on signals from global navigation satellite systems enabling measurements of the tidal range [47], [48]. 3) Flow estimation using Doppler sonar based on circular statistics [49]. 4) Determining the instantaneous angle in electrical generators [50]. 5) Phase lock-in amplifiers using circular regression for detection of weak sinusoidals in noisy signals [51]. 6) Edge detection for pattern recognition in images [52]. 7) Orientation estimation of objects in images [53]. 8) Protein structure prediction based on uncertain estimates of dihedral angles [54]. 9) Multi-target tracking for bearings-only measurements with a circular probability hypothesis density filter [55].

Deterministic sampling for purely circular state estimation has already been successfully applied in control [56] and heart phase estimation [57]. Yet most of the existing circular deterministic sampling methods are limited to particular types of density functions and particular numbers of samples. Only the "Binary Tree" sampling can get an arbitrary number of samples from any circular density where the cumulative density function (CDF) is available [17]. However, it is not invariant w.r.t. an interval choice and samples are not optimally placed.

D. Contribution

This paper presents a method to optimally approximate a continuous angular density function ${}^{\mathrm{C}}f(\underline{x})$ on the circular domain with a Dirac mixture density (DMD) ${}^{\mathrm{DM}}f(\underline{x})$ with an arbitrary number samples.

II. PROBLEM FORMULATION AND KEY IDEA

Let ${}^{\mathrm{C}}f(\underline{x})$, $\underline{x} \in S^1$, be an arbitrary continuous density function on the circle, considered as reference density here. The goal is to obtain a DMD

$$ {}^{\mathrm{DM}}f(\underline{x}) = \frac{1}{L} \sum_{i=1}^{L} \delta(\underline{x} - \hat{\underline{x}}_i) \tag{1} $$

with sample locations $\hat{\underline{x}}_i \in S^1$, $i \in \{1, 2, \ldots, L\}$. This DMD should optimally approximate the given continuous reference density, limited in accuracy only by the allowed number of samples L. Required inputs are

I1 the number L of wanted samples,
I2 a numerical function handle of the continuous angular reference density function ${}^{\mathrm{C}}f(\underline{x})$, $\underline{x} \in S^1$,
I3 and complexity trade-offs such as the number of iterations.

Obtained outputs are the sample locations $\hat{\underline{x}}_i \in S^1$, see Fig. 1 for an example.

To solve this, we propose to transfer the projected cumulative distribution (PCD) from the Euclidean space $\mathbb{R}^d$ [58], [59] to the circular domain S^1 and use it for deterministic sampling. The key idea is the projection to one-dimensional

(a) Two projected densities   (b) Projected sampling procedure   (c) Fixed eval. points   (d) Adaptive eval. points
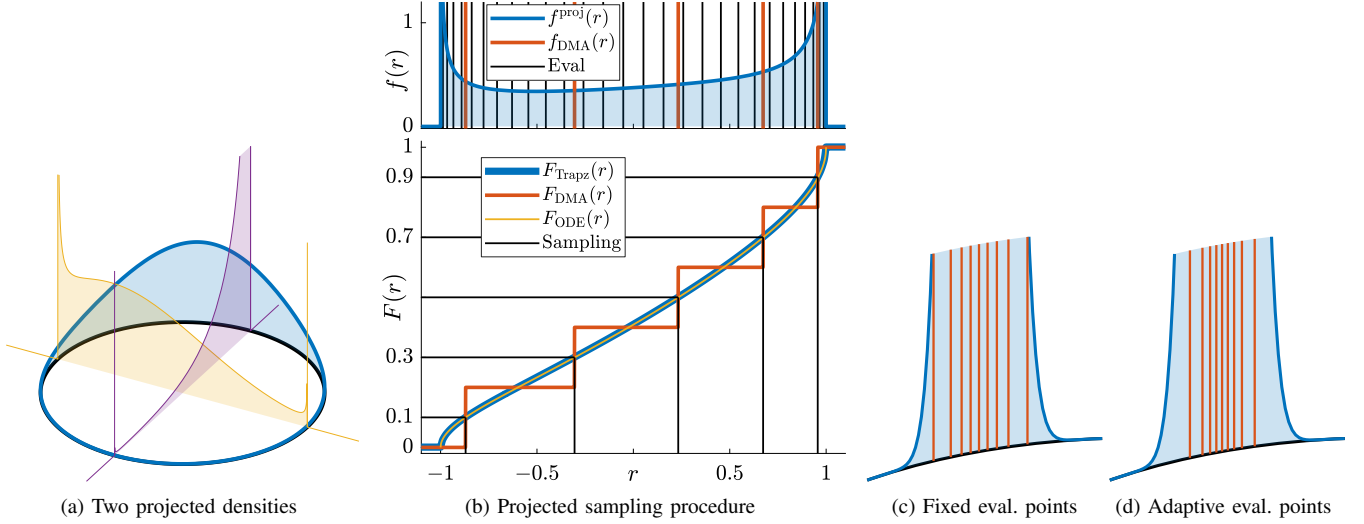
Fig. 2: **(a)** Continuous density function (blue) and two orthographic projections or marginals (yellow, purple), see (7). **(b)** Procedure for deterministic sampling of a projected von Mises-Fisher density, using orthographic projection (7). Upper part: we evaluate $f(r)$ (blue) at the fixed evaluation points t_j^{h} (black) as well as previous sample locations (red). Lower part: Trapezoidal integration on said evaluation points is performed (blue). Compare the ground truth obtained with a numerical ODE solver (yellow). Then, one-dimensional deterministic sampling is performed (black), yielding an approximating DM distribution function (red). See also Alg. 1 for a more detailed description. **(c, d)** Deterministic circular sampling using (c) only a fixed base set of 30 evaluation points t_j^{h} versus (d) the 30 fixed base points plus the previous samples, for better numerical integration. The difference for this quite "narrow" von Mises-Fisher distribution ($\kappa = 500$) is notable.

marginal distributions, thereby we reduce a multivariate problem to a set of univariate ones. In the univariate setting, cumulative distributions are uniquely defined and can easily be approximated even for arbitrary density functions. In other words, we match a continuous density with a DMD in the Radon domain [60]. To optimally capture and transfer all of the density's details, it is important to include about 50 to 100 different projections, which we implement iteratively.

III. PROJECTION OF THE CIRCULAR DOMAIN

Projection along a certain direction $\underline{u} \in S^1$ allows to compare one-dimensional PDFs $f(r|\underline{u})$ at a time. CDFs $F(r|\underline{u})$ are uniquely defined in one dimension and, if no closed-form solution is available, can easily be calculated from the PDFs via the trapezoidal rule with proposal samples. Furthermore, it is straightforward to compare two one-dimensional CDFs. The following two types of projections $f(r|\underline{u})$ of circular densities $f(\underline{x})$, (a) exponential map and (b) orthographic projection, appear to be equally performant for our purpose.

A. Exponential Map

Consider the circular domain as a real interval of length 2π by cutting the unit circle open at an arbitrary position $\underline{u} \in S^1$, and "unwrapping" it to a one-dimensional interval

$$f(r|\underline{u}) = \begin{cases} f\left(\begin{bmatrix} \cos(r - \angle\underline{u}) \\ \sin(r - \angle\underline{u}) \end{bmatrix}\right), & 0 \le r \le 2\pi, \\ 0, & \text{otherwise}, \end{cases} \quad (2)$$

where $\angle\underline{u} = \operatorname{atan2}(\underline{u}^{(2)}, \underline{u}^{(1)})$ is an angular representation of $\underline{u}$.

Intuitively, one might unwrap the circle just once at the point of lowest probability density, compute the according CDF, and place samples on the $[0, 2\pi]$ interval using inverse transform sampling, i.e., propagating equidistant samples on $[0, 1]$ through the inverse CDF. However, this works perfectly only if the density doesn't "interact" across that point of lowest density. That is, the overall density should be narrow, and virtually zero in a considerably wide region around the point of lowest density. Otherwise, all circular permutations have to be considered [61], [62]. For example, the wrapped Cauchy distribution in Fig. 3b exhibits some interaction across the point of smallest density.

B. Orthographic Projection

Consider the Euclidean embedding of the circular manifold S^1 in $\mathbb{R}^2$. We then perform a linear projection

$$\boldsymbol{r} = \underline{u}^\top \boldsymbol{x}, \quad (3)$$

of the random variable $\boldsymbol{x}$ using the direction vector $\underline{u}$, which yields a univariate random variable $\boldsymbol{r}$. In terms of densities, we calculate the marginal distribution along $\underline{u}$

$$f(r|\underline{u}) = \int_{S^1} f(\underline{x})\, \delta(r - \underline{u}^\top \underline{x})\, \mathrm{d}\underline{x} \quad | \ \alpha = \angle\underline{x} \quad (4)$$

$$= \int_{\alpha=0}^{2\pi} f\left(\begin{bmatrix} \cos(\alpha) \\ \sin(\alpha) \end{bmatrix}\right) \delta\left(r - \begin{bmatrix} \cos(\angle\underline{u}) \\ \sin(\angle\underline{u}) \end{bmatrix}^\top \begin{bmatrix} \cos(\alpha) \\ \sin(\alpha) \end{bmatrix}\right) \mathrm{d}\alpha \quad (5)$$

Algorithm 1: Calculate sample deltas that make a DMD approximate a continuous density by matching the cumulatives, in the univariate (projected) setting.

Function
$\{\Delta r_i\}_{i=1}^{L} \leftarrow$ sample1D($f_{\boldsymbol{r}}(\cdot)$, $\{r_i\}_{i=1}^{L}$)
Input: $f_{\boldsymbol{r}}(\cdot)$: continuous reference density in one dimension,
  $\{r_i\}_{i=1}^{L}$: current sample approximation
Output: $\{\Delta r_i\}_{i=1}^{L}$: proposed step for each sample, to improve similarity to $f_{\boldsymbol{r}}(\cdot)$

$\{t_i^{\mathrm{h}}\}_{i=1}^{L^{\mathrm{h}}}$ // Fixed evaluation points
$\{t_j\}_{j=1}^{L^{\mathrm{e}}=L^{\mathrm{h}}+L} \leftarrow \{t_i^{\mathrm{h}}\}_{i=1}^{L^{\mathrm{h}}} \cup \{r_i\}_{i=1}^{L}$
$\{F_j\}_{j=1}^{L^{\mathrm{e}}} \leftarrow$ cumtrapz($\{t_j\}_{j=1}^{L^{\mathrm{e}}}$, $\{f_{\boldsymbol{r}}(t_j)\}_{j=1}^{L^{\mathrm{e}}}$)
$\{F_j\}_{j=1}^{L^{\mathrm{e}}} \leftarrow \{F_j + \frac{1-F_{L^{\mathrm{e}}}}{2}\}_{j=1}^{L^{\mathrm{e}}}$ // Centering
for $i \leftarrow 1$ **to** L **do**
   $F^{\mathrm{det}} \leftarrow \frac{2i-1}{2L}$ // Deterministic sampling
   $(j^{\mathrm{L}}, j^{\mathrm{R}}) \leftarrow$ adjacent(F^{det}, $\{F_j\}_{j=1}^{L^{\mathrm{e}}}$)
   // Quadratic interpolation
   $m \leftarrow \frac{f_{j^{\mathrm{R}}} - f_{j^{\mathrm{L}}}}{t_{j^{\mathrm{R}}} - t_{j^{\mathrm{L}}}}$
   $(a,b,c) \leftarrow F_{j^{\mathrm{L}}} + \int_{t_{j^{\mathrm{L}}}}^{x} m \cdot (x - t_{j^{\mathrm{L}}}) \, \mathrm{d}x \stackrel{!}{=} F^{\mathrm{det}}$
   $(x_1^{\mathrm{quad}}, x_2^{\mathrm{quad}}) \leftarrow$ roots(a,b,c)
   // Linear interpolation
   $x^{\mathrm{lin}} \leftarrow \frac{F^{\mathrm{det}} - F_{j^{\mathrm{L}}}}{m} + t_{j^{\mathrm{L}}}$
   // Updated sample location
   $r_i^{\mathrm{e}} \leftarrow$ select_best($x_1^{\mathrm{quad}}, x_2^{\mathrm{quad}}, x^{\mathrm{lin}}$)
end
// Assign r_i and r_i^{e}
$\left(\{r_i^{\mathrm{sort}}\}_{i=1}^{L}, \{j_i\}_{i=1}^{L} \right) \leftarrow$ sort($\{r_i\}_{i=1}^{L}$)
for $i \leftarrow 1$ **to** L **do**
   $\Delta r_{j_i} \leftarrow r_i^{\mathrm{e}} - r_i^{\mathrm{sort}}$ // Sample step
end

$$= \int_{\alpha=0}^{2\pi} f\left(\begin{bmatrix} \cos(\alpha) \\ \sin(\alpha) \end{bmatrix} \right) \delta(r - \cos(\alpha - \angle \underline{u})) \, \mathrm{d}\alpha \qquad (6)$$

$$= \begin{cases} \sum_{i=1}^{2} f\left(\begin{bmatrix} \cos(\alpha_i + \angle \underline{u}) \\ \sin(\alpha_i + \angle \underline{u}) \end{bmatrix} \right) \frac{1}{|\sin(\alpha_i)|}, & |r| \le 1, \\ 0, & |r| > 1, \end{cases} \qquad (7)$$

with

$$\alpha_i = \begin{cases} \arccos(r), & i = 1, \\ 2\pi - \arccos(r), & i = 2. \end{cases} \qquad (8)$$

See Fig. 2a for a visualization of two orthographic projections of a von Mises density.

IV. IMPLEMENTATION

With a suitable projection at hand, we can now start approximating the given continuous density. It is well known that samples of any one-dimensional density, like our projected

---

Algorithm 2: PCD-based deterministic sampling of conditional circular densities.

Function $\{\hat{\underline{x}}_i\}_{i=1}^{L} \leftarrow$ sampleS1($f_{\underline{\boldsymbol{x}}}(\cdot)$, L)
Input: $f_{\underline{\boldsymbol{x}}}(\cdot)$: continuous circular density, $\underline{x} \in S^2$,
  L: number of wanted samples
Output: $\{\hat{\underline{x}}_i\}_{i=1}^{L}$: deterministic samples on the circle that approximate $f_{\underline{\boldsymbol{x}}}(\cdot)$
$N \leftarrow 2$ // Projections per iteration
// High quality for visualization
$M \leftarrow 200$ // Number of iterations
$\lambda_0 \leftarrow 0.99$ // Update step decrease factor
// Initialization
$\lambda \leftarrow 1$
$\{\hat{\underline{x}}_i\}_{i=1}^{L} \leftarrow$ rand(L, S^2)
for $m \leftarrow 1$ **to** M **do**
   $\varphi_0 \leftarrow$ rand(1, S^2)
   $\{\Delta \hat{\underline{x}}_i\}_{i=1}^{L} \leftarrow \underline{0}$
   for $n \leftarrow 1$ **to** N **do**
     // Symmetric projections
     $\varphi \leftarrow \pi \cdot (n-1)/N + \varphi_0$
     $\underline{u} \leftarrow \begin{bmatrix} \cos(\varphi) \\ \sin(\varphi) \end{bmatrix}$
     // Project the samples $\hat{\underline{x}}_i \to r_i$
     $\{r_i\}_{i=1}^{L} \leftarrow \{\underline{u}^\top \hat{\underline{x}}_i\}_{i=1}^{L}$
     // Project the density $f_{\underline{\boldsymbol{x}}}(\cdot) \to f_{\boldsymbol{r}}(\cdot|\underline{u})$
     // according to Sec. III
     $f_{\boldsymbol{r}}(\cdot) \leftarrow$ project($f_{\underline{\boldsymbol{x}}}(\cdot)$, $\underline{u}$)
     // Get projected sample updates
     // using Alg. 1
     $\{\Delta r_i\}_{i=1}^{L} \leftarrow$ sample1D($f_{\boldsymbol{r}}(\cdot)$, $\{r_i\}_{i=1}^{L}$)
     // Get sample updates in $\mathbb{R}^2$
     $\{\Delta \underline{x}_i\}_{i=1}^{L} \leftarrow \{$ backproject(Δr_i) $\}_{i=1}^{L}$
     $\{\Delta \hat{\underline{x}}_i\}_{i=1}^{L} \leftarrow \{\Delta \hat{\underline{x}}_i + \Delta \underline{x}_i\}_{i=1}^{L}$
   end
   $\lambda \leftarrow \lambda \cdot \lambda_0$
   for $i \leftarrow 1$ **to** L **do**
     // Perform sample update
     $\hat{\underline{x}}_i \leftarrow \hat{\underline{x}}_i + \lambda \Delta \hat{\underline{x}}_i / N$
     // Restrict to S^2
     $\varphi_i \leftarrow$ atan2($\hat{\underline{x}}_i^{(2)}$, $\hat{\underline{x}}_i^{(1)}$)
     $\hat{\underline{x}}_i \leftarrow \begin{bmatrix} \cos(\varphi_i) \\ \sin(\varphi_i) \end{bmatrix}$
   end
end

PDF, can easily be drawn when the inverse of the CDF is available. Therefore, we seek to obtain the following intermediate results one by one in the course of this section:

- reference PDF ${}^{\mathrm{C}}f(\underline{x})$ (is given),
- projected PDF ${}^{\mathrm{C}}f(r|\underline{u})$,
- projected CDF ${}^{\mathrm{C}}F(r|\underline{u})$,
- inverse CDF ${}^{\mathrm{C}}F^{-1}(p|\underline{u})$,
- sample locations r_i,
- sample updates $\Delta \underline{x}_i$.
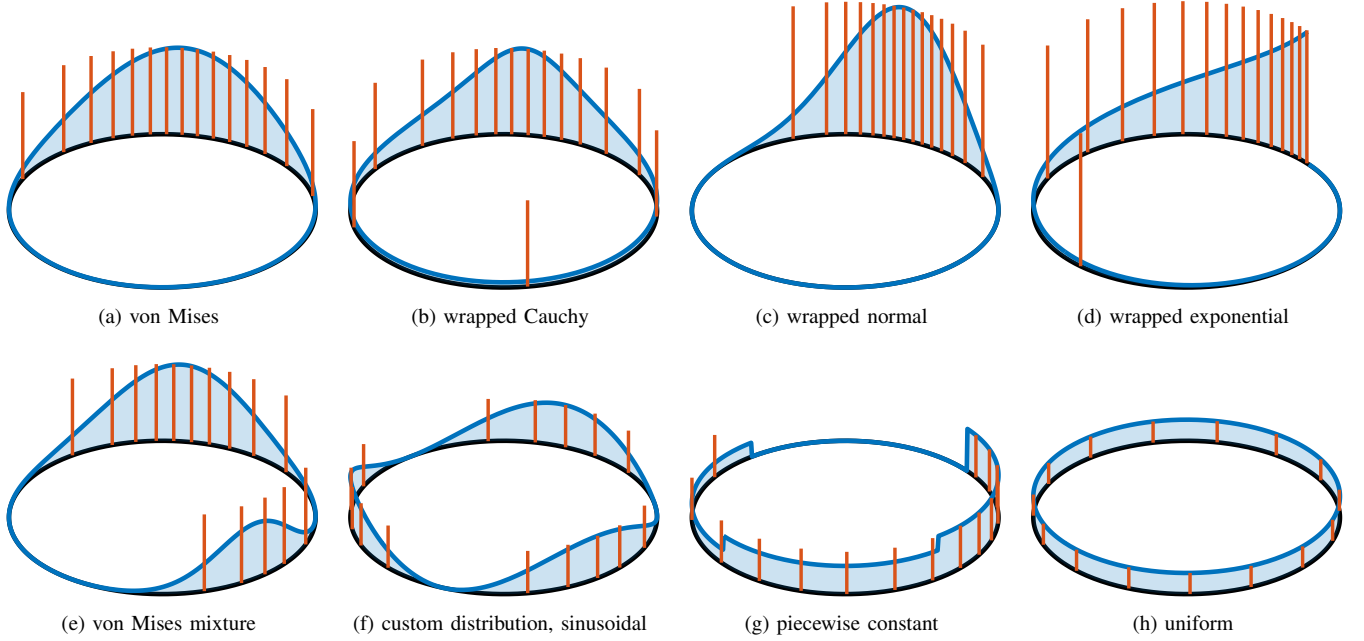
Fig. 3: Illustration of various circular distributions and deterministic samples obtained with the proposed method. Continuous probability density function (blue) on the angular domain S^1 (black), with sampling results (red). For better visualization, the length of the red lines representing the unweighted samples has been set to the maximum density function value (mode) instead of the sample weight $1/L$.

The procedure will then be repeated iteratively for different projection vectors $\underline{u}$.

A. Composite Trapezoidal Integration

The projected PDF $^\mathrm{C}f(r|\underline{u})$ is available in closed form by inserting the given $^\mathrm{C}f(\underline{x})$ into (2) or (7). Since we are permitting arbitrary density functions, a closed-form representation of the according CDF

$$^\mathrm{C}F(r|\underline{u}) = \int_{t=-\infty}^{r} f(t|\underline{u})\,\mathrm{d}t \qquad (9)$$

is not possible in general. However, we know that the integrand $f(r|\underline{u})$ has limited support, i.e., $r \in [0, 2\pi]$ for the exponential map projection (2), and $r \in [-1, 1]$ for the orthographic projection (7). To obtain an approximation of $F(r|\underline{u})$, we apply the composite trapezoidal rule with an adaptive set of function evaluation points t_j.

A fixed base set of homogeneous function evaluation points t_j^h inside the support interval is always used to ensure a good general approximation of the CDF's global shape. In addition to the base points, to maintain proper accuracy of the numerical integral even in the case of very localized PDFs with small extent, the projected samples r_i^p in the currently assumed approximating density $^\mathrm{DM}f(r|\underline{u})$ are always included into the set of function evaluation points. Summarizing, after composite trapezoidal integration of $^\mathrm{C}f(r|\underline{u})$ with said evaluation points, we now have a piecewise quadratic representation of the projected reference CDF, $^\mathrm{C}F(r|\underline{u})$.

B. Deterministic Sampling

We draw deterministic samples p_i that are uniformly distributed in $[0, 1]$,

$$p_i = \frac{2i-1}{2L}\,, \qquad i \in \{1, 2, \ldots, L\}\,, \qquad (10)$$

and propagate them through the inverse CDF to obtain deterministic samples r_i of $^\mathrm{C}f(r|\underline{u})$

$$r_i = {^\mathrm{C}F}^{-1}(p_i|\underline{u})\,, \qquad i \in \{1, 2, \ldots, L\}\,. \qquad (11)$$

Under the assumptions that have been made with the trapezoidal rule, our representation of $^\mathrm{C}f(r|\underline{u})$ is piecewise linear, and thus $^\mathrm{C}F(r|\underline{u})$ is a piecewise quadratic. Therefore, evaluation of $^\mathrm{C}F^{-1}(p_i|\underline{u})$ for any p_i to obtain r_i involves two steps. First, a search for the relevant interval, i.e., an adjacent pair $(t_\mathrm{L}, t_\mathrm{R})$ from the trapezoidal function evaluation points t_i such that $^\mathrm{C}F(t_\mathrm{L}|\underline{u}) \leq p_i < {^\mathrm{C}F}(t_\mathrm{R}|\underline{u})$. Second, the quadratic (or sometimes linear) function that represents the CDF in this segment has to be inverted, which is easily done in closed form.

Of course, if a closed-form representation of the projected CDF or even its inverse is available, we can use it directly for sampling, with no need for trapezoidal integration. For example, a fast approximation of the von Mises-Fisher density's cumulative (in conjunction with the exponential map) is available in closed form [63]. Note that deterministic sampling by propagating equally distributed deterministic samples, i.e., equidistant samples, on $[0,1]$ through the inverse CDF, as proposed here, is equivalent to deterministic sampling

| (a) Mean estimate versus L | (b) Run time versus L | (c) Error versus run time |
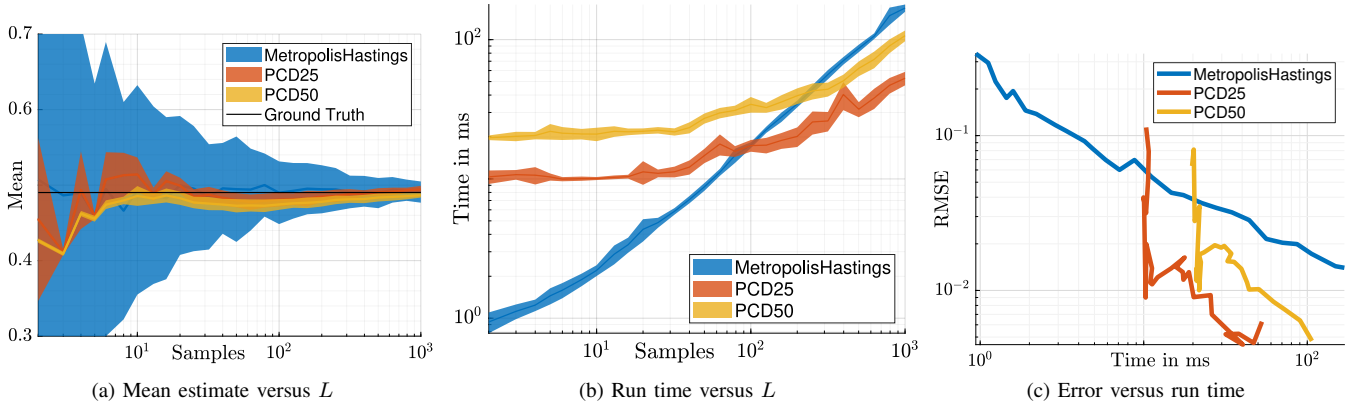
Fig. 4: Evaluation that compares the proposed deterministic PCD sampling with 25 iterations (red) and 50 iterations (yellow) to random sampling (blue). Shaded areas denote 1σ-bounds based on 100 trials. **(a)** Expectation value estimation with nonlinear function (12). **(b)** Computation time needed to obtain L samples. **(c)** Optimality plot showing estimation error versus computational complexity for sampling only.

by minimizing the L^2-norm of the difference of both CDFs [58].

At this point, we have available the deterministic sample locations r_i in the projected space that is defined by the projection direction $\underline{u}$. See Fig. 2b for a visualization of CDF-based sampling in the projected space.

C. Sample Update

The projected sample locations r_i now have to be back-projected to the original domain S^1. We typically use updates from several symmetrically arranged projections simultaneously in order not to create preferential directions. The projected samples generated as described in Sec. IV-B are not naturally associated with the existing samples from previous iterations. Thus, we have to find an appropriate association first. Projection also helps us here as in the one-dimensional case, the association that minimizes the global distance of associated point pairs can simply be obtained by element-wise comparison of the sorted sets. The according global distance is also called Wasserstein distance. Refer to Alg. 1 for a pseudo-code representation of the procedure described up to here.

D. Multiple Projections

To equally consider all dimensions, we propose to use a symmetric set of N projections in each iteration step. For the case $N = 2$ as considered here, we use $N = 2$ projections per iteration. We choose orthogonal projections (90° between them) but with random orientation, see Fig. 2a for an example. The individual sample updates from each projection are averaged, thus yielding the total update $\Delta\underline{\hat{x}}_i$ of the current iteration step.

E. Iterative Update

The procedure is repeated until the arrangement of the samples obtains a satisfactory quality. In practice, one can specify a fixed number of iterations like 10, 25, or 50 –

depending on how locally homogeneous and accurate the points should be. In general, the trade-off between the number of samples and the number of iterations depends on the computational complexity of the algorithm that uses the generated samples afterwards. To asymptotically reach a stationary state, we propose to multiply sample updates with an exponentially decreasing discounting factor λ. This accounts for the fact that more and more information (from more projections) is already present in the sample locations and the amount of extra information provided by every additional iteration decreases. Refer to Alg. 2 for a more detailed presentation regarding the iterative sample update scheme.

V. EVALUATION

Our adaptive choice of evaluation points for numerical integration allows for an accurate approximation even for "narrow" densities, see Fig. 2d, where the base set of fixed evaluation points alone would not be sufficient, see Fig. 2c. Note that acceptance-rejection random sampling with a uniform proposal would be very inefficient in this case. The flexibility of the proposed method is demonstrated by showing obtained deterministic samples from various density functions, see Fig. 3.

A simulation of a nonlinear expectation value estimation demonstrates the capabilities of our proposed method more quantitatively. We compare the proposed deterministic sampling with random samples from the Metropolis-Hastings method [1] using the implementation in the libDirectional library [64]. It samples from arbitrary density functions, just like our proposed new method. An equally distributed initial sampling set is transformed to a von Mises density ($\mu = 0, \kappa = 3$) in 25 and 50 iterations, respectively, with two projections per iteration, and a base set of 30 fixed evaluation points t_j^{h} for the composite trapezoidal rule. The expected value of

$$\boldsymbol{z} = \sqrt{(\boldsymbol{x} - 1)^2 + \boldsymbol{y}^2} \tag{12}$$

is estimated based on these samples. See Fig. 4 for the results. Estimation accuracy is of course much better with deterministic samples than with random samples, see Fig. 4a. The cost is however more computation time, although PCD sampling can get faster than Metropolis-Hastings for $L > t_j^{\mathrm{h}}$, see Fig. 4b. Note that PCD sampling becomes even more attractive when the nonlinear function propagating the samples is computationally complex because PCD means fewer samples for the same accuracy.

MATLAB source code implementing the presented algorithm is published as supplementary material in IEEE Xplore as a Code Ocean capsule[1].

VI. Conclusions

We presented a new, alternative method for generating any number of deterministic samples for any continuous density function on the circle. The concept can be applied just as well in higher dimensions. It does not require gradient-based numerical optimization like LCD-based methods. Instead, we use a naturally gradient-free method to optimize sample locations iteratively. Moreover, the distance measure is simple and indisputable: fitting the cumulatives in terms of the L^2 norm is always an adequate solution for univariate densities. No parameters such as kernel widths or weighting functions need to be chosen. Using PCD, we can apply the same elementary method (fitting one-dimensional cumulatives) to higher dimensions. Our proposed solution is faster than existing methods based on the LCD, yet it still requires an iterative loop to get optimal sample locations. Therefore it is especially suitable 1) when function evaluations in the calculation of expected values are relatively expensive, e.g., require their own simulation, and evaluation points must be chosen as carefully as possible, or 2) where the deterministic sampling results can be pre-calculated offline and stored in a static library for online use.

In the future, we will extend this method to higher-dimensional geometries such as the hypersphere and the hypertorus. While calculating the projected densities was straightforward on the circle, it will be more difficult in higher dimensions, because one-dimensional cumulatives have to be calculated repeatedly when using the PCD method. We will look for closed-form solutions that work for specific types of densities. Furthermore, numerical integration techniques with an adaptive choice of evaluation points will be pursued, as also pure sample reduction techniques, where no integration is necessary. Presumably, orthographic projection is a good choice for hyperspherical higher-dimensional extensions of the circle, and the exponential map for the Cartesian product of circles, i.e., toroidal manifolds.

References

[1] W. K. Hastings, "Monte Carlo Sampling Methods Using Markov Chains and Their Applications," *Biometrika*, vol. 57, no. 1, pp. 97–109, 04 1970.

[2] G. Kurz and U. D. Hanebeck, "Stochastic Sampling of the Hyper-spherical von Mises–Fisher Distribution Without Rejection Methods," in *Proceedings of the IEEE ISIF Workshop on Sensor Data Fusion: Trends, Solutions, Applications (SDF 2015)*, Bonn, Germany, Oct. 2015.

[3] B. D. Flury, "Acceptance–Rejection Sampling Made Easy," *SIAM Review*, vol. 32, no. 3, pp. 474–476, 1990.

[4] D. Frisch and U. D. Hanebeck, "Rejection Sampling from Arbitrary Multivariate Distributions Using Generalized Fibonacci Lattices," in *Proceedings of the 25th International Conference on Information Fusion (Fusion 2022)*, Linköping, Sweden, July 2022.

[5] M. Simandl, J. Královec, and T. Söderström, "Advanced Point-Mass Method for Nonlinear State Estimation," *Automatica*, vol. 42, no. 7, pp. 1133–1145, 2006.

[6] G. Kurz, F. Pfaff, and U. D. Hanebeck, "Discrete Recursive Bayesian Filtering on Intervals and the Unit Circle," in *Proceedings of the 2016 IEEE International Conference on Multisensor Fusion and Integration for Intelligent Systems (MFI 2016)*, Baden-Baden, Germany, Sep. 2016.

[7] F. Pfaff, K. Li, and U. D. Hanebeck, "The Spherical Grid Filter for Nonlinear Estimation on the Unit Sphere," in *Proceedings of the 1st Virtual IFAC World Congress (IFAC-V 2020)*, Jul. 2020.

[8] ——, "Estimating Correlated Angles Using the Hypertoroidal Grid Filter," in *Proceedings of the 2020 IEEE International Conference on Multisensor Fusion and Integration for Intelligent Systems (MFI 2020)*, Virtual, Sep. 2020.

[9] T. Li, S. Sun, J. M. Corchado, T. P. Sattar, and S. Si, "Numerical Fitting-Based Likelihood Calculation to Speed up the Particle Filter," *International Journal of Adaptive Control and Signal Processing*, vol. 30, no. 11, pp. 1583–1602, 2016.

[10] F. Pfaff, G. Kurz, and U. D. Hanebeck, "Multivariate Angular Filtering Using Fourier Series," *Journal of Advances in Information Fusion*, vol. 11, no. 2, pp. 206–226, Dec. 2016. [Online]. Available: https://confcats_isif.s3.amazonaws.com/web-files/journals/entries/JAIF_Vol11_2_7.pdf

[11] K. Ito and K. Xiong, "Gaussian Filters for Nonlinear Filtering Problems," *IEEE Transactions on Automatic Control*, vol. 45, no. 5, pp. 910–927, 2000.

[12] S. J. Julier and J. K. Uhlmann, "New Extension of the Kalman Filter to Nonlinear Systems," in *Signal Processing, Sensor Fusion, and Target Recognition VI*, vol. 3068. International Society for Optics and Photonics, Jul. 1997, pp. 182–193.

[13] S. J. Julier, "The Scaled Unscented Transformation," in *Proceedings of the 2002 American Control Conference (IEEE Cat. No.CH37301)*, vol. 6, May 2002, pp. 4555–4559 vol.6.

[14] G. Kurz, I. Gilitschenski, and U. D. Hanebeck, "Recursive Nonlinear Filtering for Angular Data Based on Circular Distributions," in *Proceedings of the 2013 American Control Conference (ACC 2013)*, Washington D.C., USA, Jun. 2013.

[15] ——, "Nonlinear Measurement Update for Estimation of Angular Systems Based on Circular Distributions," in *Proceedings of the 2014 American Control Conference (ACC 2014)*, Portland, Oregon, USA, Jun. 2014.

[16] ——, "Recursive Bayesian Filtering in Circular State Spaces," *IEEE Aerospace and Electronic Systems Magazine*, vol. 31, no. 3, pp. 70–87, Mar. 2016.

[17] G. Kurz, I. Gilitschenski, R. Y. Siegwart, and U. D. Hanebeck, "Methods for Deterministic Approximation of Circular Densities," *Journal of Advances in Information Fusion*, vol. 11, no. 2, pp. 138–156, Dec. 2016. [Online]. Available: https://confcats_isif.s3.amazonaws.com/web-files/journals/entries/JAIF_Vol11_2_3.pdf

[18] I. Gilitschenski, G. Kurz, S. J. Julier, and U. D. Hanebeck, "Unscented Orientation Estimation Based on the Bingham Distribution," *IEEE Transactions on Automatic Control*, vol. 61, no. 1, pp. 172–177, Jan. 2016.

[19] G. Kurz, I. Gilitschenski, and U. D. Hanebeck, "Unscented von Mises–Fisher Filtering," *IEEE Signal Processing Letters*, vol. 23, no. 4, pp. 463–467, Apr. 2016.

[20] G. Kurz and U. D. Hanebeck, "Deterministic Sampling on the Torus for Bivariate Circular Estimation," *IEEE Transactions on Aerospace and Electronic Systems*, vol. 53, no. 1, pp. 530–534, Feb. 2017.

[21] K. Li, F. Pfaff, and U. D. Hanebeck, "Hyperspherical Unscented Particle Filter for Nonlinear Orientation Estimation," in *Proceedings of the 1st Virtual IFAC World Congress (IFAC-V 2020)*, Jul. 2020.

[22] ——, "Unscented Dual Quaternion Particle Filter for SE(3) Estimation," *IEEE Control Systems Letters*, vol. 5, no. 2, pp. 647–652, Apr. 2021. [Online]. Available: https://doi.org/10.1109/LCSYS.2020.3005066

[23] M. Brossard, S. Bonnabel, and J. Condomines, "Unscented Kalman Filtering on Lie Groups," in *2017 IEEE/RSJ International Conference on Intelligent Robots and Systems (IROS)*, 2017, pp. 2485–2491.

[24] S. Hauberg, F. Lauze, and K. S. Pedersen, "Unscented Kalman Filtering on Riemannian Manifolds," *Journal of Mathematical Imaging and Vision*, vol. 46, no. 1, pp. 103–120, May 2013.

[25] H. M. T. Menegaz, J. Y. Ishihara, and H. T. M. Kussaba, "Unscented Kalman Filters for Riemannian State-Space Systems," *IEEE Transactions on Automatic Control*, vol. 64, no. 4, pp. 1487–1502, 2019.

[26] A. J. Izenman, "Recent Developments in Nonparametric Density Estimation," *Journal of the American Statistical Association*, vol. 86, no. 413, pp. 205–224, 1991.

[27] U. D. Hanebeck and V. Klumpp, "Localized Cumulative Distributions and a Multivariate Generalization of the Cramér-von Mises Distance," in *Proceedings of the 2008 IEEE International Conference on Multisensor Fusion and Integration for Intelligent Systems (MFI 2008)*, Seoul, Republic of Korea, Aug. 2008, pp. 33–39.

[28] U. D. Hanebeck, "Optimal Reduction of Multivariate Dirac Mixture Densities," *at – Automatisierungstechnik, Oldenbourg Verlag*, vol. 63, no. 4, pp. 265–278, Apr. 2015. [Online]. Available: https://dx.doi.org/10.1515/auto-2015-0005

[29] J. Steinbring and U. D. Hanebeck, "LRKF Revisited: The Smart Sampling Kalman Filter (S2KF)," *Journal of Advances in Information Fusion*, vol. 9, no. 2, pp. 106–123, Dec. 2014. [Online]. Available: https://confcats_isif.s3.amazonaws.com/web-files/journals/entries/441_1_art_11_17020.pdf

[30] D. Frisch and U. D. Hanebeck, "Efficient Deterministic Conditional Sampling of Multivariate Gaussian Densities," in *Proceedings of the 2020 IEEE International Conference on Multisensor Fusion and Integration for Intelligent Systems (MFI 2020)*, Virtual, Sep. 2020.

[31] K. Li, D. Frisch, B. Noack, and U. D. Hanebeck, "Geometry-Driven Deterministic Sampling for Nonlinear Bingham Filtering," in *Proceedings of the 2019 European Control Conference (ECC 2019)*, Naples, Italy, Jun. 2019.

[32] K. Li, F. Pfaff, and U. D. Hanebeck, "Hyperspherical Deterministic Sampling Based on Riemannian Geometry for Improved Nonlinear Bingham Filtering," in *Proceedings of the 22nd International Conference on Information Fusion (Fusion 2019)*, Ottawa, Canada, Jul. 2019.

[33] D. Frisch, K. Li, and U. D. Hanebeck, "Optimal Reduction of Dirac Mixture Densities on the 2-Sphere," in *Proceedings of the 1st Virtual IFAC World Congress (IFAC-V 2020)*, Jul. 2020.

[34] K. Li, F. Pfaff, and U. D. Hanebeck, "Hyperspherical Dirac Mixture Reapproximation," *arXiv preprint arXiv:2110.10411*, Oct. 2021. [Online]. Available: https://arxiv.org/abs/2110.10411

[35] ——, "Dual Quaternion Sample Reduction for SE(2) Estimation," in *Proceedings of the 23rd International Conference on Information Fusion (Fusion 2020)*, Virtual, Jul. 2020.

[36] ——, "Nonlinear von Mises–Fisher Filtering Based on Isotropic Deterministic Sampling," in *Proceedings of the 2020 IEEE International Conference on Multisensor Fusion and Integration for Intelligent Systems (MFI 2020)*, Virtual, Sep. 2020.

[37] ——, "Progressive von Mises–Fisher Filtering Using Isotropic Sample Sets for Nonlinear Hyperspherical Estimation," *Sensors*, Apr. 2021. [Online]. Available: https://www.mdpi.com/1424-8220/21/9/2991

[38] A. T. Hayes, A. Martinoli, and R. M. Goodman, "Distributed Odor Source Localization," *IEEE Sensors Journal*, vol. 2, no. 3, pp. 260–271, 2002.

[39] J.-G. Li, Q.-H. Meng, Y. Wang, and M. Zeng, "Odor Source Localization Using a Mobile Robot in Outdoor Airflow Environments With a Particle Filter Algorithm," *Autonomous Robots*, vol. 30, no. 3, pp. 281–292, Apr 2011.

[40] Y. Ban, X. Alameda-Pineda, C. Evers, and R. Horaud, "Tracking Multiple Audio Sources With the von Mises Distribution and Variational EM," *IEEE Signal Processing Letters*, vol. 26, no. 6, pp. 798–802, 2019.

[41] C. Evers, E. A. P. Habets, S. Gannot, and P. A. Naylor, "DoA Reliability for Distributed Acoustic Tracking," *IEEE Signal Processing Letters*, vol. 25, no. 9, pp. 1320–1324, 2018.

[42] C. Evers, H. W. Löllmann, H. Mellmann, A. Schmidt, H. Barfuss, P. A. Naylor, and W. Kellermann, "The LOCATA Challenge: Acoustic Source Localization and Tracking," *IEEE/ACM Transactions on Audio, Speech, and Language Processing*, vol. 28, pp. 1620–1643, 2020.

[43] G. Stienne, S. Reboul, M. Azmani, J. Choquel, and M. Benjelloun, "A Multi-Temporal Multi-Sensor Circular Fusion Filter," *Information Fusion*, vol. 18, pp. 86–100, 2014.

[44] K. Li, D. Frisch, S. Radtke, B. Noack, and U. D. Hanebeck, "Wavefront Orientation Estimation Based on Progressive Bingham Filtering," in *Proceedings of the IEEE ISIF Workshop on Sensor Data Fusion: Trends, Solutions, Applications (SDF 2018)*, Oct. 2018.

[45] S. Bultmann, K. Li, and U. D. Hanebeck, "Stereo Visual SLAM Based on Unscented Dual Quaternion Filtering," in *Proceedings of the 22nd International Conference on Information Fusion (Fusion 2019)*, Ottawa, Canada, Jul. 2019.

[46] G. Stienne, S. Reboul, J. Choquel, and M. Benjelloun, "Cycle Slip Detection and Repair With a Circular on-Line Change-Point Detector," *Signal Processing*, vol. 100, pp. 51–63, 2014.

[47] T. Hobiger, R. Haas, and J. Löfgren, "Software-Defined Radio Direct Correlation GNSS Reflectometry by Means of GLONASS," *IEEE Journal of Selected Topics in Applied Earth Observations and Remote Sensing*, vol. 9, no. 10, pp. 4834–4842, 2016.

[48] J. Strandberg, T. Hobiger, and R. Haas, "Improving GNSS-R Sea Level Determination Through Inverse Modeling of SNR Data," *Radio Science*, vol. 51, no. 8, pp. 1286–1296, 2016.

[49] G. Fromant, G. Stienne, and S. Reboul, "Circular Estimation of the Flow Velocity Using Coherent Doppler Sonar," in *2020 IEEE 23rd International Conference on Information Fusion (FUSION)*, 2020, pp. 1–6.

[50] P. Tripathy, S. C. Srivastava, and S. N. Singh, "A Divide-by-Difference-Filter Based Algorithm for Estimation of Generator Rotor Angle Utilizing Synchrophasor Measurements," *IEEE Transactions on Instrumentation and Measurement*, vol. 59, no. 6, pp. 1562–1570, 2010.

[51] G. Wang, S. Reboul, J.-B. Choquel, E. Fertein, and W. Chen, "Circular Regression in a Dual-Phase Lock-In Amplifier for Coherent Detection of Weak Signal," *Sensors*, vol. 17, no. 11, 2017.

[52] A. P. James, "Edge Detection for Pattern Recognition: A Survey," *International Journal of Applied Pattern Recognition*, vol. 3, no. 1, pp. 1–21, 2016.

[53] F. Pfaff, K. Li, and U. D. Hanebeck, "Deep Likelihood Learning for 2-D Orientation Estimation Using a Fourier Filter," in *Proceedings of the 24th International Conference on Information Fusion (Fusion 2021)*, Sun City, South Africa, Nov. 2021.

[54] M. Shapovalov and R. Dunbrack, "A Smoothed Backbone-Dependent Rotamer Library for Proteins Derived from Adaptive Kernel Density Estimates and Regressions," *Structure*, vol. 19, no. 6, pp. 844–858, 2011.

[55] I. Marković, J. Ćesić, and I. Petrović, "Von Mises Mixture PHD Filter," *IEEE Signal Processing Letters*, vol. 22, no. 12, pp. 2229–2233, 2015.

[56] G. Kurz, M. Dolgov, and U. D. Hanebeck, "Nonlinear Stochastic Model Predictive Control in the Circular Domain," in *Proceedings of the 2015 American Control Conference (ACC 2015)*, Chicago, Illinois, USA, Jul. 2015.

[57] G. Kurz and U. D. Hanebeck, "Heart Phase Estimation Using Directional Statistics for Robotic Beating Heart Surgery," in *Proceedings of the 18th International Conference on Information Fusion (Fusion 2015)*, Washington D.C., USA, Jul. 2015.

[58] U. D. Hanebeck, "Deterministic Sampling of Multivariate Densities based on Projected Cumulative Distributions," in *Proceedings of the 54th Annual Conference on Information Sciences and Systems (CISS 2020)*, Princeton, New Jersey, USA, Mar. 2020.

[59] D. Prossel and U. D. Hanebeck, "Dirac Mixture Reduction Using Wasserstein Distances on Projected Cumulative Distributions," in *Proceedings of the 25th International Conference on Information Fusion (Fusion 2022)*, Linköping, Sweden, July 2022.

[60] J. Radon, "Über die Bestimmung von Funktionen durch ihre Integralwerte längs gewisser Mannigfaltigkeiten," *Berichte über die Verhandlungen der Sächsische Akademie der Wissenschaften*, vol. 69, pp. 262–277, 1917, 00000.

[61] H. C. Shen and A. K. C. Wong, "Generalized Texture Representation and Metric," *Computer Vision, Graphics, and Image Processing*, vol. 23, no. 2, pp. 187–206, Aug. 1983. [Online]. Available: https://www.sciencedirect.com/science/article/pii/0734189X83901123

[62] M. Werman, S. Peleg, R. Melter, and T. Y. Kong, "Bipartite Graph Matching for Points on a Line or a Circle," *Journal of Algorithms*, vol. 7, no. 2, pp. 277–284, Jun. 1986. [Online]. Available: https://www.sciencedirect.com/science/article/pii/019667748690009X

[63] G. W. Hill, "Algorithm 518: Incomplete Bessel Function I_0. The Von Mises Distribution [S14]," *ACM Trans. Math. Softw.*, vol. 3, no. 3, p. 279–284, Sep. 1977.

[64] G. Kurz, I. Gilitschenski, F. Pfaff, L. Drude, U. D. Hanebeck, R. Haeb-Umbach, and R. Y. Siegwart, "Directional Statistics and Filtering Using libDirectional," *Journal of Statistical Software*, May 2019. [Online]. Available: https://dx.doi.org/10.18637/jss.v089.i04